

Integral backstepping integral sliding mode control of underactuated nonlinear electromechanical systems

S. Ullah*, Q. Khan**, A. Mehmood*,
R. Akmeliawati***

**Department of Electrical & Computer Engineering, COMSATS University, Islamabad, Pakistan (e-mail: safeer_iui@yahoo.com, adeel.mehmood@comsats.edu.pk).*

***Center for Advanced Studies in Telecommunication (CAST), COMSATS University, Islamabad, Pakistan (e-mail: qudratullah@comsats.edu.pk)*

****School of Mechanical Engineering, The University of Adelaide, Adelaide SA 5005, Australia, (e-mail: rini.akmeliawati@adelaide.edu.au)*

Abstract: This paper presents an integral backstepping integral sliding mode (IBISMC) based robust control scheme to asymptotically stabilize a class of underactuated nonlinear electromechanical systems (UNEMSs) at desired equilibria. Prior to the control design, the dynamic model of the aforesaid class is first transformed into a regular form which is more convenient for control design. This transformation subdivides the overall system's dynamics into a series cascaded form which are termed as internal dynamics and visible dynamics blocks while proceeding from the left side. A proportional integral based nonlinear virtual control laws are designed in a backstep manner and an integral sliding mode is introduced in the last step of the design. In this way, the overall system is controlled via a robust nonlinear control algorithm which results in zero steady state errors in each step and also provides robustness against step disturbances and matched uncertainties. The global asymptotic stability of each step is proved via Lyapunov candidate function. The applicability and benefits of this strategy are demonstrated via the simulation results of a cart-pendulum system. The results of the proposed strategy are also compared with the standard literature results to highlight its appealing nature for such class.

Keywords: Underactuated systems, cart-pendulum, integral backstepping, integral sliding mode control.

1. INTRODUCTION

Mechanical systems that are characterized by the fact that they have less dimension of space spanned by the applied stabilizing inputs than that of the space spanned by the configuration variables are called underactuated systems (ud Din et al., 2018). This class has very interesting applications in the field of robotics, unmanned aerial vehicles, underwater vehicles, surface vessels, satellite and locomotive systems (Gruszka et al., 2011; Khan et al., 2017; Huang and Yan, 2017; Ghommam et al., 2006; Spong et al., 2007). Moreover, this class offers certain advantages like reduction in energy consumption, cost, weight and the sufficiently low failure rate of their components. Because of its substantial applications in the existing era, the nonlinear control design of the underactuated nonlinear electromechanical systems has been the key focus of the researchers during the recent decades (see for instance, Fantoni and Lozano, 2002; Lu et al., 2018; Nafa et al., 2013). As reported in Riachy et al. (2008), the smooth control approaches may not be applied to control the UNEMSs because of the existence of some nonintegrable constraints with some theoretical and practical challenges (Berkemeier and Fearing, 1999, Zhang and Tarn, 2002). In the context of advanced control algorithms, an extensive number of researchers synthesized different nonlinear control techniques to provide appealing results

along with closed-loop stability. Some of these efforts are reported here.

A passivity-based control (PBC) scheme, utilized the entire power, in a considerable range to acquire the equilibrium values for the system dynamics which are very often needed in stabilization problems (Romeo et al., 1998; Fierro et al., 1999). Many researchers have successively employed the PBC scheme for the set-point regulation of UNEMSs, for example, bipedal locomotion robot in (Spong et al., 2007), translational oscillator with rotational actuator (TORA) in (Jankovic et al., 1996), etc. The conservativeness of this technique lied in the facts that its range of realistic implementation in the field of robotics and aerospace engineering is so limited. In addition, it was only valid for the stability of those systems which display relative degree one. To overcome the limitation of relative degree one, a nonlinear control technique, known as backstepping, is proposed. It converts the n th order system into a new recursive form that contained on n number of subsystems (each one of relative degree one). In recent years, this control scheme is mostly used for the global stabilization of the UNEMSs, like unmanned aerial vehicle in (Gruszka et al., 2011), spacecraft in (Huang and Yan, 2017) and surface vessel in (Ghommam et al., 2006). Unfortunately, when the degrees of freedom of the aforesaid class increases then the design procedure of such a control scheme becomes very

complex and it is very difficult to employ it in a realistic application. An energy-optimal control scheme, reported in (Yang et al., 2011), solved the problem of energy consumption of system dynamics. A differential geometric based time optimal control approach is used to control the nonholonomic rigid systems along with some specific application, like the planar pendulum in (Mason et al., 2008) and spacecraft in (Tsiotras and Luo, 2000). However, the main shortcoming of (Mason et al., 2008; Tsiotras and Luo, 2000) was that they had no generalized rules for the control of UNEMSs. An artificial intelligent control technique, the so-called fuzzy logic control (FLC), deal with imprecise, uncertain and qualitative decision-making problems. It has been extensively utilized in the practical application of UNEMSs (see for instance (Tao et al., 2008; Li et al., 2004)). FLC is of two types: model-based FLC and heuristics-based FLC. In model-based FLC scheme, the regulation of setpoints and output tracking on the desired trajectory are presented in (Ichida et al., 2006; Raguraman et al., 2009), respectively. The combination of FLC with some other control approaches have some excellent results in the presence of mismatched uncertainties (Nafa et al., 2013; Aloui et al., 2011; Hwang et al., 2009). However, the limitations in the existing results of FLC are pointed out that: 1). the dynamic variables of systems are required to be established in advance, which is often unavailable in a practical scenario, 2). the rule failures of fuzzy inference occur due to the intersected conflicting decision boundaries.

In the context of robust nonlinear control schemes employment, the sliding mode control (SMC) is extensively applied in the presence of internal and external uncertainties (Soysal, 2014). It finds very interesting results in controlling the dynamics of UNEMSs, such as cart-pendulum system in (Riachy et al., 2008), UAV in (Zou, 2017), ball and beam system in (Din et al., 2017; Almutairi and Zribi, 2010), satellite in (Huang and Yan, 2017) and double-pendulum crane in (Lee et al., 2013). However, due to the presence of strong dynamics coupling and high nonlinear terms in UNEMSs, the chattering phenomena becomes more prominent (Bartoszewicz, 2017). To overcome this problem, multifarious classical and advanced control strategies are employed (see for instance, (Lee and Utkin, 2007; Benallegue et al., 2008; Vazquez et al., 2014; Din et al., 2017; ud Din et al., 2018; Bartolini et al., 1998; Levant, 2003)). The control algorithms developed in (Din et al., 2017; ud Din et al., 2018) were quite appealing but it suffered from less precision because of asymptotic convergence with a steady-state error. For higher precessions, a fast terminal sliding mode control (TSMC) approach (Khan et al., 2017) is presented to compensate the chattering problems. This approach not only achieves finite-time convergence in the sliding phase but also provided better robustness in comparison with traditional linear SMC along with high precision (presented in (Xiong and Zheng, 2014)). However, the existence of negative fractional powers in TSMC may lead to singularity problems (Zhao et al., 2015) and it also experiences the reaching phase which is often proved sensitive to disturbances.

It is necessary to report that the development of the integral backstepping based integral sliding mode strategy for the understudy class is based on some motivations. The integral backstepping results in zero steady state errors as compared to conventional backstepping. In addition, integral backstepping also improves the robustness against the disturbance of step type. On the other hand, the integral sliding mode is introduced in the last step of the design to provide us the invariance property (an important property of sliding modes) from the very start as compared to conventional sliding modes which guarantee invariance only in sliding phase. In other words, the reaching phase is eliminated the system evolves in sliding mode from the very start which ensures robustness from the very start. Furthermore, this strategy results in suppressed chattering as compared to conventional sliding modes.

The main objectives met in this work are three fold. At first, some transformations are made to convert the dynamic model, of a class of UNEMSs, into regular form. This facilitates the design of the proposed control law. Secondly, the employment of integral backstepping strategy to the transformed regular form in a very generic way subject to very practical assumptions. An integral sliding mode is developed in the last step which helps in getting rid of the reaching phase. Consequently, the system evolves with more robustness from the start of the process as compared to conventional sliding modes and conventional nonlinear techniques. The closed lope stability in each step is proved via Lyapunov stability theory. The chattering phenomena is also alleviated via strong reachability condition as well as by the introduction of the integral sliding mode which generally results in reduced chattering (see for more details, (Utkin, 1999)). Thirdly, the effectiveness of the proposed algorithm is demonstrated via the simulation results of a cart-pendulum and its transient and steady state responses are compared with the second order sliding mode control strategy (Riachy et al., 2008). In addition, a quantitative comparison is also made with the above referred in table 1. The rest of the paper is structured as follows: the problem statement is presented in Section 2 and a generalized integral backstepping based ISM control design is given in Section 3. The proposed control scheme is verified while simulating a benchmark cart-pendulum system in Section 4. The last Section includes the conclusion followed by references.

2. PROBLEM FORMULATION

The most general form of the dynamics of uncertain nonlinear mechanical system, in vector form, is expressed as

$$J(p)\ddot{p} + F_c(p, \dot{p})\dot{p} + F_g(p) + F_b(\dot{p}) = F_e(p)U + \Delta_p \quad (1)$$

where $J \in \mathbb{R}^{n \times n}$ is a non-singular inertia matrix, $p \in \mathbb{R}^{n \times 1}$ and $\dot{p} \in \mathbb{R}^{n \times 1}$ are the position and velocity vectors which makes a configuration space of $2n$ variables, the force matrices $F_g(p)$, $F_b(\dot{p})$ and $F_c(p, \dot{p})$ are known as gravitational, fractional, and centrifugal/Coriolis forces, respectively (see

(Olfati-Saber, 2001), for more details). In addition, $U \in \mathbb{R}^{n \times 1}$ is the applied control input, $F_e \in \mathbb{R}^{n \times n}$ denotes the matrix of external forces and $\Delta_p = \Delta_p(p, \dot{p}, t)$ refers to the lumped uncertainty contributed by the coupling of the states, external disturbances and unmodeled dynamics.

The general model (1) for 2-DOF underactuated nonlinear electromechanical systems, can be written as follows

$$\begin{aligned} \ddot{p}_1 &= M_{11}(p_1, p_2, \dot{p}_1, \dot{p}_2) + M_{12}(p_1, p_2)(U + \Delta_{p1}(p_1, p_2, t)) \\ \ddot{p}_2 &= M_{21}(p_1, p_2, \dot{p}_1, \dot{p}_2) + M_{22}(p_1, p_2)(U + \Delta_{p2}(p_1, p_2, t)) \end{aligned} \quad (2)$$

where $M_{11}(p_1, p_2, \dot{p}_1, \dot{p}_2)$ and $M_{21}(p_1, p_2, \dot{p}_1, \dot{p}_2)$ represents combinations of centrifugal, Coriolis, gravitational and fractional forces, $M_{12}(p_1, p_2)$ and $M_{22}(p_1, p_2)$ are the channels of the feedback control input U . Furthermore, $\Delta_{p1}(p_1, p_2, t)$ and $\Delta_{p2}(p_1, p_2, t)$ represents the state dependent nonlinear uncertain coupling terms.

Using non-singular coordinate transformation (reported in (Utkin et al., 2009)), the above generalized UNEMSS model (2) is transformed to following the equivalent regular form:

$$\begin{aligned} \ddot{r} &= H_1(r, \dot{r}, q, \dot{q}) \\ \ddot{q} &= H_2(r, \dot{r}, q, \dot{q}) + G_2(r, q)U + \tilde{\Delta}(r, q, t) \end{aligned} \quad (3)$$

where $q = p_2$ and $\dot{q} = \dot{p}_2$, $r = \mathcal{G}(p_1, p_2) = p_1 - \mathcal{G}(p_2)$, $\dot{r} = \dot{p}_1 - \frac{\partial}{\partial p_2} \mathcal{G}(p_2) \dot{p}_2$, $\frac{\partial}{\partial p_2} \mathcal{G}(p_2) = \frac{M_{12}}{M_{22}}$,

$$\ddot{r} = \ddot{p}_1 - \frac{\partial}{\partial p_2} \left(\frac{\partial}{\partial p_2} \mathcal{G}(p_2) \dot{p}_2 \right) \dot{p}_2 = H_1(r, \dot{r}, q, \dot{q}),$$

$$\begin{aligned} H_2(r, \dot{r}, q, \dot{q}) &= M_{21}(p_1, p_2, \dot{p}_1, \dot{p}_2) \quad \text{and} \\ G_2(r, q) &= M_{22}(p_1, p_2). \end{aligned}$$

It is worthy to mention that $H_1(r, \dot{r}, q, \dot{q})$, $H_2(r, \dot{r}, q, \dot{q})$ and $G_2(r, q)$ are smooth functions. It is also necessary to report that since the overall system is controllable therefore, $G_2(r, q)$ should not be zero in the feasible domain (in the working domain).

At this stage, we assume the following.

Assumption 1. It is assumed that the uncertainty $\tilde{\Delta}(r, q, t)$ is the norm bounded i.e., $|\tilde{\Delta}| \leq \lambda$, where λ is a positive constant.

Remark 1. Note that, the transformation does not alter the nature of the matched uncertainty.

The transformed model (3), in state space variable form, can be re-written as

$$\begin{cases} \dot{x}_1 = x_2 \\ \dot{x}_2 = H_1(x_1, x_2, x_3, x_4) \\ \dot{x}_3 = x_4 \\ \dot{x}_4 = H_2(x_1, x_2, x_3, x_4) + G_2(x_1, x_3)U + \tilde{\Delta}(x_1, x_3, t) \end{cases} \quad (4)$$

where $x_1 = r_1$, $x_3 = q_1$, $\dot{x}_1 = \dot{r}_1$ and $\dot{x}_3 = \dot{q}_1$. Before the control design, the following assumptions are also made.

Assumption 2. The equilibrium point of an open loop system is assumed to be at the origin, such that $H_1(0, 0, 0, 0) = 0$ and $H_2(0, 0, 0, 0) = 0$.

Assumption 3. For a feasible practical scenario, assume that the nonlinear function H_1 depends only on the position variable of the directly driven system i.e., $H_1(x_1, x_2, x_3, x_4) = H_1(x_1, x_2, x_3, 0)$.

The structure in Assumption (3) is mostly observed in underactuated nonlinear systems such as an inverted-pendulum system in (Khan et al., 2017), double-inverted pendulum system in (Utkin et al., 2009) and TORA system in (Olfati-Saber, 2001).

Assumption 4. Assume that the function $H_1(x_1, x_2, x_3, 0)$ can be subdivided into the following form $H_1(x_1, x_2, x_3, 0) = H_{11}(x_1, x_2, x_3)H_{12}(x_3)$, where $H_{11}(x_1, x_2, x_3, 0)$ remains positive and inactive in the available feasible domain (see (Khan et al., 2017) in case inverted pendulum and (Utkin et al., 2009) in case of double inverted pendulum). Thus, the main interest here is that $H_{12}(x_3)$ must be no-vanishing and invertible.

Assumption 5. Assume that the control input channel $G_2(x_1, x_3) \in \mathbb{R}^{m \times m}$ should be a nonvanishing (i.e., invertible in the whole domain). In other words, it is needed that $G_2(x_1, x_3) \neq 0 \quad \forall x_1$ and $x_3 \in \mathbb{R}$ to maintain controllability.

Now, the overall problem is formulated in which the main objective is to steer all the states of (4) to the equilibrium points. In the next section, an integral backstepping based ISMC law is proposed to meet the steering objective.

3. CONTROL LAW DESIGN

The design of the control law via integral backstepping ISMC is the main topic of this section. In the control design steps, the system (4) is interpreted in the following two cases which will ease the understanding and development of the design.

3.1 case-I

The first two multi-variable differential equations in (4) are analogous to internal dynamics whose zero dynamics, with x_3 as an output, can be obtained by substituting $x_3 = 0$ and $x_4 = 0$, as follows

$$\begin{aligned}\dot{x}_1 &= x_2 \\ \dot{x}_2 &= H_1(x_1, x_2, 0, 0)\end{aligned}\quad (5)$$

When the internal dynamics (5) are stable, then the ultimate task is that the following dynamics, under the action of a suitably designed, control input U should follow the desired reference output.

$$\begin{aligned}\dot{x}_3 &= x_4 \\ \dot{x}_4 &= H_2(x_1, x_2, x_3, x_4) + G_2(x_1, x_3)U + \tilde{\Delta}(x_1, x_3, t)\end{aligned}\quad (6)$$

This tracking task can be met by steering the mismatch ε_3 between the real output x_3 and the reference output x_{3r} (which is assumed continuously differentiable) to zero. Therefore, proceeding towards the control design, the mismatch is defined as

$$\varepsilon_3 = x_3 - x_{3r}\quad (7)$$

The differentiation of the Lyapunov function $\Lambda_3 = \varepsilon_3^2 / 2$ along (7) yields

$$\dot{\Lambda}_3 = \varepsilon_3 \dot{\varepsilon}_3 = \varepsilon_3(x_4 - \dot{x}_{3r})\quad (8)$$

Choosing a virtual controller ($x_4^* = \dot{x}_{3r} - \kappa_3 \varepsilon_3$) and a new reference ($x_4^* = \dot{x}_{3r} - \kappa_3 \varepsilon_3 - \eta_3 \chi_3$): with $\chi_3 = \int \varepsilon_3 dt$, the time derivative of the Lyapunov function will become

$$\dot{\Lambda}_3 = -\kappa_3 \varepsilon_3^2 + \varepsilon_3 \varepsilon_4 - \eta_3 \varepsilon_3 \chi_3\quad (9)$$

where κ_3 is the positive control gain and $\varepsilon_4 = x_4 - x_4^*$ is the mismatch for the next step. The steering of ε_4 exponentially at zero can be obtained by defining an integral sliding manifold σ of the form

$$\sigma = x_4 - x_4^* + z: \text{ where } z = \int_0^t \varepsilon_4 d\tau\quad (10)$$

The time derivative of σ along (6) takes the form

$$\begin{aligned}\dot{\sigma} &= H_2(x_1, x_2, x_3, x_4) + G_2(x_1, x_3)U + \tilde{\Delta}(x_1, x_3, t) \\ &\quad - \ddot{x}_{3r} + \kappa_3(\varepsilon_4 - \kappa_3 \varepsilon_3) + \eta_3 \varepsilon_3 + \dot{z}\end{aligned}\quad (11)$$

In this strategy, the control law is considered to be an algebraic sum of two components, i.e., $U = U_0 + U_1$, where U_0 is a continuous control component and U_1 is further composed of U_{dis} and U_{eq} terms. The term \dot{z} is chosen as follows

$$\dot{z} = -G_2(x_1, x_3)U_0: \text{ where } U_0 = -\eta_4(x_4 - x_4^*)\quad (12)$$

Consequently, (11) becomes

$$\begin{aligned}\dot{\sigma} &= H_2(x_1, x_2, x_3, x_4) + G_2(x_1, x_3)U_1 + \tilde{\Delta}(x_1, x_3, t) \\ &\quad - \ddot{x}_{3r} + \kappa_3(\varepsilon_4 - \kappa_3 \varepsilon_3) + \eta_3 \varepsilon_3\end{aligned}\quad (13)$$

The differentiation of an augmented Lyapunov function $\Lambda_4 = \Lambda_3 + \sigma^2 / 2 + \eta_3 \chi_3^2 / 2$ along (9) and (11) becomes

$$\begin{aligned}\dot{\Lambda}_4 &= -\kappa_3 \varepsilon_3^2 + \varepsilon_3 \varepsilon_4 + \sigma(H_2(x_1, x_2, x_3, x_4) - \ddot{x}_{3r} \\ &\quad + G_2(x_1, x_3)U_1 + \tilde{\Delta}(x_1, x_3, t) + \kappa_3(\varepsilon_4 - \kappa_3 \varepsilon_3) + \eta_3 \varepsilon_3)\end{aligned}\quad (14)$$

To ensure regularization, the equivalent control law U_{eq} is designed as

$$\begin{aligned}U_{eq} &= \frac{1}{G_2(x_1, x_3)}(-H_2(x_1, x_2, x_3, x_4) + \ddot{x}_{3r} \\ &\quad - \kappa_3(\varepsilon_4 - \kappa_3 \varepsilon_3) - \eta_3 \varepsilon_3)\end{aligned}\quad (15)$$

and the discontinuous control law is devised as

$$U_{dis} = \frac{1}{G_2(x_1, x_3)}(-\kappa_4(\sigma + \kappa_5 \text{sign}(\sigma))\quad (16)$$

Considering (15) and (16), the applied control law U_1 is designed as

$$\begin{aligned}U_1 &= \frac{1}{G_2(x_1, x_3)}(-H_2(x_1, x_2, x_3, x_4) + \ddot{x}_{3r} \\ &\quad - \kappa_3(\varepsilon_4 - \kappa_3 \varepsilon_3) - \kappa_4(\sigma + \kappa_5 \text{sign}(\sigma)) - \eta_3 \varepsilon_3)\end{aligned}\quad (17)$$

Invoking the control laws (17), Eq. (14) becomes

$$\begin{aligned}\dot{\Lambda}_4 &\leq -\kappa_3 \varepsilon_3^2 + \varepsilon_3 \varepsilon_4 - \kappa_4 \sigma^2 - |\sigma|(\kappa_4 \kappa_5 - |\tilde{\Delta}|) \\ \dot{\Lambda}_4 &\leq -\kappa_3 \varepsilon_3^2 + \varepsilon_3 \varepsilon_4 - \kappa_4 \sigma^2 - \lambda |\sigma|\end{aligned}\quad (18)$$

where λ is a positive constant. This inequality remains a true subject to $\kappa_4 \kappa_5 \geq |\tilde{\Delta}(x_1, x_3, t)| + \lambda$. The controller (17) enforces sliding mode from the very start of the process which means $\sigma = 0$ is met at $t = 0$. The constraint $\sigma = 0$ implies that $\dot{\varepsilon}_4 + G_2(x_1, x_3)U_0 = 0$. This shows that the uncertain and nonlinear terms are compensated by the control component U_1 and the nominal system in term of ε_4 , in sliding mode, is governed by U_0 . The solution of this differential equation is exponentially converging to origin i.e., $\varepsilon_4 \rightarrow 0$ exponentially under the action of U_0 . This shows that the second term in the inequality (18) will vanish and it confirms the negative definiteness of the right side of (18).

3.2 case-II

In the case-I, the stability of the zero dynamics with x_3 as an output is discussed. Now, in this case, the stability of the zero

dynamics with x_1 as an output will be studied which can be obtained by selecting $x_1(t) = 0$ and $x_2(t) = 0$ i.e.,

$$H_1(0, 0, x_3, \dot{x}_3) = 0 \quad (19)$$

If the first order differential equation in (19) is stable, then subject to Assumption 3, the nonlinear function $H_{12}(x_3) = 0$ will be treated as a driving force of the internal dynamics block. The control law which will be designed is based on integral backstepping integral sliding mode, therefore, by defining an output tracking error ε_1 between the real output x_1 and the reference output x_r , one may get

$$\varepsilon_1 = x_1 - x_r \quad (20)$$

The differentiation of candidate Lyapunov function $\Lambda_1 = \varepsilon_1^2 / 2$ w.r.t time is presented as

$$\dot{\Lambda}_1 = \varepsilon_1 \dot{\varepsilon}_1 = \varepsilon_1(x_2 - \dot{x}_r) \quad (21)$$

Treating x_2 as a virtual controller and choosing a new reference ($x_2^* = \dot{x}_r - \kappa_1 \varepsilon_1 - \eta_1 \chi_1$): with $\chi_1 = \int_0^t \varepsilon_1 d\tau$, the time derivative of the Lyapunov function will become

$$\dot{\Lambda}_1 = -\kappa_1 \varepsilon_1^2 + \varepsilon_1 \varepsilon_2 - \eta_1 \varepsilon_1 \chi_1 \quad (22)$$

where κ_1 is the positive control gain and $\varepsilon_2 = x_2 - x_2^*$ is the mismatch for the next step. The differentiation of ε_2 along system (4) (subject to Assumption 4) can be defined

as follows

$$\begin{aligned} \dot{\varepsilon}_2 &= \dot{x}_2 - \ddot{x}_r + \kappa_1 \dot{\varepsilon}_1 \\ \dot{\varepsilon}_2 &= H_{11}(x_1, x_2, x_3)H_{11}(x_3) - \ddot{x}_r + \kappa_1(\varepsilon_2 - \kappa_1 \varepsilon_1) \end{aligned} \quad (23)$$

For the convergence of error variables ε_1 and ε_2 to zero, the time derivative of the Lyapunov function

$\Lambda_2 = \Lambda_1 + \varepsilon_2^2 / 2 + \eta_1 \chi_1^2 / 2$ along (22) and (23) becomes

$$\begin{aligned} \dot{\Lambda}_2 &= -\kappa_1 \varepsilon_1^2 + \varepsilon_2(\varepsilon_1 + H_{11}(x_1, x_2, x_3)H_{12}(x_3) \\ &\quad - \ddot{x}_r + \kappa_1(\varepsilon_2 - \kappa_1 \varepsilon_1)) \end{aligned} \quad (24)$$

From Eq. (24), a virtual control input is designed, to enforce x_2 to x_2^* , as follows

$$x_3^* = H_{12}^{-1} \left\{ \begin{aligned} &H_{11}^{-1}(x_1, x_2, x_3)(-\varepsilon_1 - \kappa_1(\varepsilon_2 - \kappa_1 \varepsilon_1)) \\ &+ \ddot{x}_r - \kappa_2 \varepsilon_2 - \eta_2 \chi_2 \end{aligned} \right\} \quad (25)$$

which yields

$$\dot{\Lambda}_2 = -\kappa_1 \varepsilon_1^2 - \kappa_2 \varepsilon_2^2 + \varepsilon_2 \varepsilon_3 - \eta_2 \varepsilon_2 \chi_2 \quad (26)$$

Since the actual driving force U is appearing in the second block that can be accessed by defining a mismatch ε_3 between the real output x_3 and the reference output x_3^* i.e.,

$$\varepsilon_3 = x_3 - x_3^* \quad (27)$$

The differentiation of the Lyapunov function $\Lambda_3 = \Lambda_2 + \varepsilon_3^2 / 2 + \eta_2 \chi_2^2 / 2$ along (27), yields

$$\dot{\Lambda}_3 = -\kappa_1 \varepsilon_1^2 - \kappa_2 \varepsilon_2^2 + \varepsilon_3(x_4 - \dot{x}_3^* + \varepsilon_2) \quad (28)$$

Once again, treating x_4 as a virtual controller and selecting a new reference ($x_4^* = \dot{x}_3^* + \varepsilon_2 - \kappa_3 \varepsilon_3 - \eta_3 \chi_3$): with $\chi_3 = \int_0^t \varepsilon_3 d\tau$, the time derivative of the Lyapunov function will become

$$\dot{\Lambda}_3 = -\kappa_1 \varepsilon_1^2 - \kappa_2 \varepsilon_2^2 - \kappa_3 \varepsilon_3^2 + \varepsilon_3 \varepsilon_4 - \eta_3 \varepsilon_3 \chi_3 \quad (29)$$

where κ_3 is the positive control gain and $\varepsilon_4 = x_4 - x_4^*$ is the mismatch for the last step. The steering of ε_4 exponentially at zero can be obtained by defining an integral sliding manifold σ of the form

$$\sigma = x_4 - x_4^* + z = x_4 - \dot{x}_3^* + \varepsilon_2 + \kappa_3 \varepsilon_3 + \eta_3 \chi_3 + z \quad (30)$$

Now, the actual control input U is reached whose design and stability of the closed loop system will be accomplished in the forthcoming theorem.

Remark 2. The nonlinear control law which will enforce sliding mode against (30) will ensure that $\varepsilon_4 = x_4 - x_4^* \rightarrow 0$. Consequently, the expression (28) will become true which will confirm the convergence of $\varepsilon_3 = x_3 - x_3^* \rightarrow 0$. Similarly, moving at backstep will confirm, at the last step, the convergence of $\varepsilon_1 = x_1 - x_r \rightarrow 0$. At this stage, the actual output will be tracking the reference even in the presence of uncertainties in the applied input channel.

Theorem 1. The step by step convergence, reported in Remark 2, can be obtained if the following control law enforces sliding mode against the integral manifold defined in (30).

$$\begin{aligned} U_1 &= \frac{1}{G_2(x_1, x_3)} (-H_2(x_1, x_2, x_3, x_4) + \dot{x}_3^* - \dot{\varepsilon}_2 \\ &\quad - \kappa_3(\varepsilon_4 - \kappa_3 \varepsilon_3) - \kappa_4(\sigma + \kappa_5 \text{sign}(\sigma)) - \eta_3 \varepsilon_3) \end{aligned} \quad (31)$$

Proof. To prove the theorem (i.e., the enforcement of sliding mode), we proceed by considering the time derivative of σ , reported in (30), along the dynamics of (6), one has

$$\begin{aligned} \dot{\sigma} &= H_2(x_1, x_2, x_3, x_4) + G_2(x_1, x_3)U + \tilde{\Delta}(x_1, x_3, t) \\ &- \dot{x}_3^* + \dot{\varepsilon}_2 + \kappa_3(\varepsilon_4 - \kappa_3\varepsilon_3) + \eta_3\varepsilon_3 + \dot{z} \end{aligned} \quad (32)$$

Since the control law is considered to be an algebraic sum of two components, i.e., $U = U_0 + U_1$. The choice of \dot{z} as follows

$$\dot{z} = -G_2(x_1, x_3)U_0: \text{ where } U_0 = -\eta_4(x_4 - x_4^*) \quad (33)$$

which leads to

$$\begin{aligned} \dot{\sigma} &= H_2(x_1, x_2, x_3, x_4) + G_2(x_1, x_3)U_1 + \tilde{\Delta}(x_1, x_3, t) \\ &- \dot{x}_3^* + \dot{\varepsilon}_2 + \kappa_3(\varepsilon_4 - \kappa_3\varepsilon_3) + \eta_3\varepsilon_3 \end{aligned} \quad (34)$$

Substituting (31) in (34), one has

$$\dot{\sigma} = -\kappa_4(\sigma + \kappa_5 \text{sign}(\sigma)) + \tilde{\Delta}(x_1, x_3, t) \quad (35)$$

Now considering the differentiation of an augmented Lyapunov function $\Lambda_4 = \Lambda_3 + \sigma^2 / 2 + \eta_3\chi_3^2 / 2$ along (35), one gets

$$\begin{aligned} \dot{\Lambda}_4 &\leq -\kappa_1\varepsilon_1^2 - \kappa_2\varepsilon_2^2 - \kappa_3\varepsilon_3^2 + \varepsilon_3\varepsilon_4 - \sigma(\kappa_4(\sigma \\ &+ \kappa_5 \text{sign}(\sigma)) - \tilde{\Delta}(x_1, x_3, t)) \\ \dot{\Lambda}_4 &\leq -\kappa_1\varepsilon_1^2 - \kappa_2\varepsilon_2^2 - \kappa_3\varepsilon_3^2 + \varepsilon_3\varepsilon_4 - \kappa_4\sigma^2 \\ &- |\sigma|(\kappa_4\kappa_5 - |\tilde{\Delta}|) \\ \dot{\Lambda}_4 &\leq -\kappa_1\varepsilon_1^2 - \kappa_2\varepsilon_2^2 - \kappa_3\varepsilon_3^2 + \varepsilon_3\varepsilon_4 - \kappa_4\sigma^2 - \lambda|\sigma| \end{aligned} \quad (36)$$

where λ is a positive constant. This inequality remains true subject to $\kappa_4\kappa_5 \geq |\tilde{\Delta}(x_1, x_3, t)| + \lambda$. The controller (31) enforces sliding mode from the very start of the process which means $\sigma = 0$ is met at $t = 0$. The constraint $\sigma = 0$ implies that $\dot{\varepsilon}_4 + G_2(x_1, x_3)U_0 = 0$. This shows that the uncertain and nonlinear terms are compensated by the control component U_1 and the nominal system in term of ε_4 , in sliding mode, is governed by U_0 . The solution of this differential equation is exponentially converging to origin i.e., $\varepsilon_4 \rightarrow 0$ exponentially under the action of U_0 . This shows that the fourth term in the inequality (36) will vanish and it confirms the negative definiteness of the right side of (36). This proves the sliding mode enforcement and the back-step regulation of the mismatches at each step.

Remark 3. Note that, in this design, the authors have designed the virtual control laws (both in case-I and case-II) by integral backstepping which will result in improved transient dynamics as well as reduced steady state errors. In the final stage of the controller, the controller is designed via the integral sliding mode strategy which confirms sliding mode from the very start. In other words, this result in enhanced robustness which, consequently, proves the plant insensitive to disturbances which often cause instability in the reaching

phase of conventional SMC. Thus, the proposed methodology is very much appealing for the control design of underactuated nonlinear electromechanical systems.

Now, in the next section, a counter example of a cart-pendulum system is considered to clarify the design strategy and to demonstrate its effectiveness in term of simulations results.

4. EXAMPLE OF CART-PENDULUM SYSTEM

4.1 System description

The cart-pendulum system is presented as a benchmark example of UNEMSS which have one input and two outputs. The pole of the inverted pendulum freely swings about the pivot point, while, on the other hand, the cart can move on the horizontal plane. Consider the following uncertain dynamics of the aforesaid system.

$$\begin{aligned} \ddot{x} &= \frac{1}{\Xi}(-mg \cos \theta \sin \theta) + \frac{4}{3} \frac{1}{\Xi}U + \Delta_x(x, \theta, t) \\ \ddot{\theta} &= \frac{1}{l\Xi}(M+m)g \sin \theta - \frac{\cos \theta}{l\Xi}U + \Delta_\theta(x, \theta, t) \end{aligned} \quad (37)$$

Where $\Xi = \frac{4}{3}(M+m) - m \cos^2 x_3$, $U = u + ml\dot{\theta}^2 \sin \theta$ u is the applied control input, l is the rod length, g is the gravitational acceleration, m is the mass of rod and M is the mass of cart. As mentioned in Section 2, the coordinate transformation will convert the dynamics of the cart-pendulum system (37) into the following equivalent regular form

$$\begin{aligned} \dot{x}_1 &= x_2 \\ \dot{x}_2 &= \left(\frac{g}{\Xi} \left(\left(\frac{4}{3} - \cos^2 x_3 \right) + \frac{4}{3}M \right) + \frac{4}{3} \frac{lx_4^2}{\cos x_3} \right) \tan x_3 \\ \dot{x}_3 &= x_4 \\ \dot{x}_4 &= \frac{1}{l\Xi} \left((M+m)g \sin x_3 \right) + \frac{\cos x_3}{l\Xi}U + \tilde{\Delta}(x_1, x_3, t) \end{aligned} \quad (38)$$

where $x_1 = x$, $x_2 = \dot{x}$, $x_3 = \theta$ and $x_4 = \dot{\theta}$. Note that this model follows all the characteristics of the Case-II. Now, the cart-pendulum system (38) is ready for the control scheme presented in section 3.

4.2 Controller design

Now the control design, via integral backstepping ISMC, is carried out by defining a miss-matched between the reference position x_r and the real position x_1 of the cart, as follows

$$\varepsilon_1 = x_1 - x_r \quad (39)$$

For positioning x_1 at the desired reference x_r , treating x_2 as a virtual control input, the new reference x_2^* is defined as

$$x_2^* = \dot{x}_r - \kappa_1 \varepsilon_1 - \eta_1 \chi_1 \tag{40}$$

In the second step, again treating x_3 as a virtual control input to steer $\varepsilon_2 = x_2 - x_2^*$ to zero. Consequently, another new reference x_3^* is designed as follows

$$x_3^* = \tan^{-1} \left\{ \frac{1}{\left(\frac{g}{\Xi} \left(\left(\frac{4}{3} - \cos^2 x_3 \right) + \frac{4}{3} M \right) + \frac{4}{3} \frac{l x_4^2}{\cos x_3} \right)} (\ddot{x}_r - \varepsilon_1 - \kappa_1(\varepsilon_2 - \kappa_1 \varepsilon_1) - \kappa_2 \varepsilon_2 - \eta_2 \chi_2) \right\} \tag{41}$$

Similarly, a new virtual control input x_4^* is defined to enforce $\varepsilon_3 = x_3 - x_3^*$ at zero with the following new reference

$$(x_4^* = x_3^* + \varepsilon_2 - \kappa_3 \varepsilon_3 - \eta_3 \chi_3) \tag{42}$$

For steering of $\varepsilon_4 = x_4 - x_4^*$ at zero in the presence of matched uncertainties $\tilde{\Delta}(x_1, x_3, t)$, a robust control law will be designed which will enforce sliding mode against the following the integral sliding manifold

$$\sigma = x_4 - x_4^* + z$$

The relevant integral dynamic appears as follows

$$\dot{z} = \frac{\cos x_3}{l \Xi} U_0 \tag{43}$$

The control law ($u = U_0 + U_{eq} + U_{dis} - mlx_4^2 \sin x_3$) for the overall dynamics comes out to be

$$u = -\frac{1}{\cos x_3} \{ l \Xi (\ddot{x}_3^* - \dot{\varepsilon}_2 - \kappa_3(\varepsilon_4 - \kappa_3 \varepsilon_3) - \eta_3 \varepsilon_3 - \kappa_4(\sigma + \kappa_5 \text{sign}(\sigma))) - (M + m) g \sin x_3 \} - \eta_4 (x_4 - x_4^*) - mlx_4^2 \sin x_3 \tag{44}$$

This control input u will provide us the benefits and results reported in Case-II. The block diagram of the proposed control scheme is depicted in the adjacent figure 1.

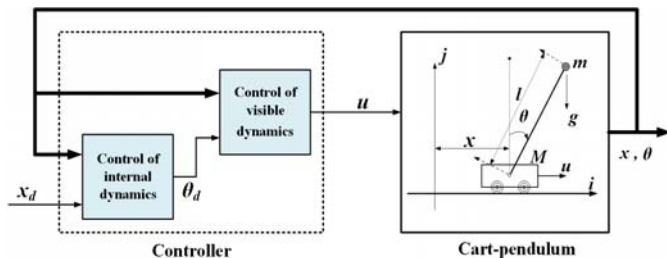


Fig. 1. Diagram of the cart-pendulum system.

Now, the MATLAB/Simulink simulation results will be presented in forthcoming subsection to demonstrate the effectiveness of the proposed control scheme.

4.3 Results discussion

In this section, the simulation results are performed via the proposed control scheme in comparison with (Riachy et al., 2008) in MATLAB/Simulink environment. The experiment is evaluated to control the dynamics of the cart-pendulum system via a nonlinear integral backstepping ISM control technique in the presence of perturbation $\tilde{\Delta}(x_1, x_3, t) = x_1 + 3 \sin x_3$ which is matched in nature. The values of the typical parameters of the cart-pendulum system are chosen to be: $m = 0.23 \text{ kg}$, $g = 9.81 \text{ m/s}^2$, $M = 2.5 \text{ kg}$ and $l = 0.36 \text{ m}$. The initial conditions and reference values of the system's states $[x_1 \ x_2 \ x_3 \ x_4]$ are given by $[0.2 \ 0 \ 45 \ 0]$ and $[0 \ 0 \ 0 \ 0]$, respectively. The values of virtual controller and actual controller gains are set to $\kappa_1 = 5.65$, $\kappa_2 = 2.65$, $\kappa_3 = 4.35$, $\kappa_4 = 2.09$ and $\kappa_5 = 0.003$ on trial and error procedure.

Figure 2 depicts the asymptotic stabilization of cart position. It is obvious that the proposed control law regulation is quite fast with far appealing precision as compared to the results of (Riachy et al., 2008). Similarly, the tracking of the rod angle at the upright position is shown in figure 3.

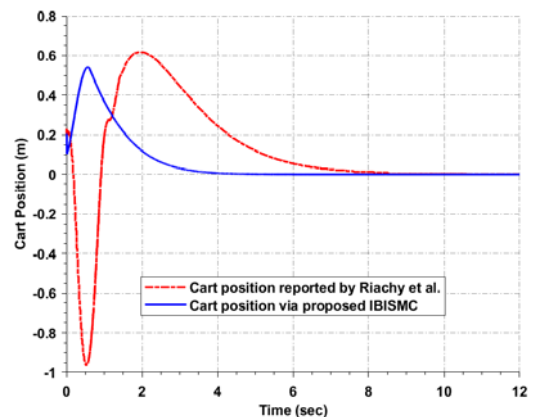


Fig. 2. The plot of linear cart position compared with the standard literature result of (Riachy et al., 2008).

The rod angle stabilization at the equilibrium via the proposed control scheme is far interesting and practical as compared to its counterpart (Riachy et al., 2008). Both the figures 2 and 3 show that the transient response of the proposed control scheme is quite fast with minimum overshoots and settling time than that in (Riachy et al., 2008). In addition, the proposed method offers zero steady state error subject to step disturbances because of the proportional integral type surface and also because of the integral backstepping scheme. Furthermore, the convergences of the system trajectories are unaffected by the matched uncertainty and the system quickly approaches the equilibrium. This confirms the robustness of the new strategy.

The control efforts of both strategies are displayed in figure 4. It is clear that the control effort of the newly proposed

technique experiences no chattering phenomenon and behaves in a very feasible manner. In other words, the results of (Riachy et al., 2008) suffers from substantial chattering which causes damage to the systems in practical implementations. Moreover, IBISMC significantly attenuated the high frequency oscillations while the control scheme in (Riachy et al., 2008) could not handled this problem efficiently. Hence, it is evident from the figures 2-4 of the cart-pendulum system that the proposed stabilizing law offers a very appealing dynamic response for a class of underactuated nonlinear electromechanical systems (that can be converted to regular form). A detailed quantitative comparison between the proposed strategy and that of (Riachy et al., 2008) is made in table 1.

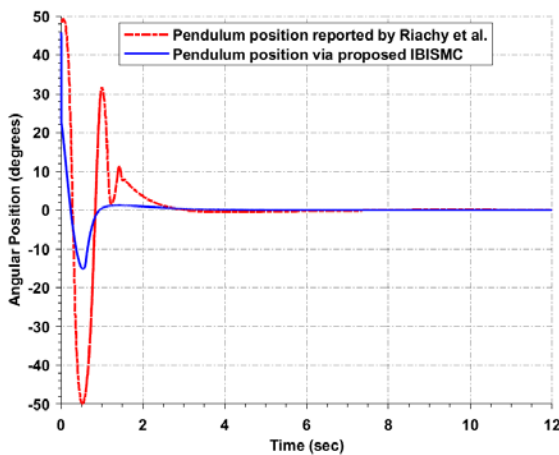


Fig. 3. The plot of angular pendulum position compared with standard literature result of (Riachy et al., 2008).

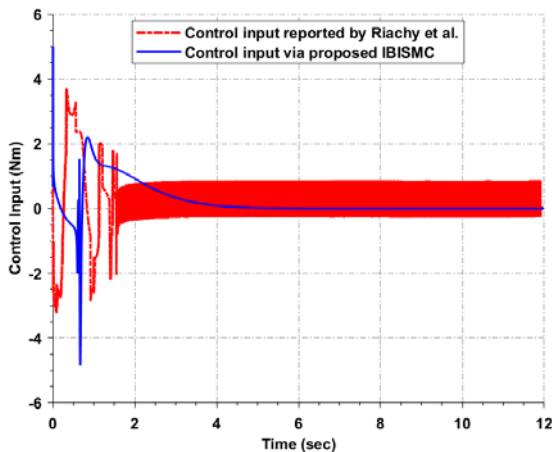


Fig. 4. The plot of control inputs compared with the standard literature result of (Riachy et al., 2008).

Table 1. stabilization results comparison

Parameter	Cart-Position		Pendulum-Position	
	SOSMC	IBISMC	SOSMC	IBISMC
Rise time (s)	0.1663	2.7753	0.1283	0.1813
Settling time (s)	8.752	3.1214	2.5847	2.0427
Peak time (s)	0.5192	0.5630	0.5291	0
Peak overshoot	0.6159	0.5477	45.8366	45.8366
Peak undershoot	-0.952	-0.56e5	-49.96	-17.09

5. CONCLUSION

A highly states coupled class of underactuated nonlinear system was considered in this paper. Prior to control design, a proper regular form conversion was presented and then a step by step integral backstepping control design was carried out in two interesting cases while taking care of the zero dynamics. The stability at each step was confirmed via Lyapunov stability approach. In the final step, an integral surfaced based robust integral sliding mode control law was designed. Finally, a cart-pendulum system was simulated in an uncertain scenario and the provided results were compared with the existing literature results of (Riachy et al., 2008). The results confirmed that our designed strategy is an appealing candidate for underactuated nonlinear electromechanical systems.

REFERENCES

Almutairi, N.B. and Zribi, M. (2010). On the sliding mode control of a ball on a beam system. *Nonlinear dynamics*, 59(1-2), 221.

Aloui, S., Pages, O., Elhajjaji, A., Chaari, A., and Koubaa, Y. (2011). Robust adaptive fuzzy sliding mode control design for a class of mimo underactuated system. In *IFAC World Congress, Milano, Italy*, 11127-11132.

Bartolini, G., Ferrara, A., and Usai, E. (1998). Chattering avoidance by second-order sliding mode control. *IEEE Transactions on automatic control*, 43(2), 241-246.

Bartoszewicz, A. (Ed.). (2017). *Recent Developments in Sliding Mode Control: Theory and Applications*. BoD-Books on Demand.

Benallegue, A., Mokhtari, A., & Fridman, L. (2008). High order sliding mode observer for a quadrotor UAV. *International Journal of Robust and Nonlinear Control: IFAC Affiliated Journal*, 18(4-5), 427-440.

Berkemeier, M.D. and Fearing, R.S. (1999). Tracking fast inverted trajectories of the underactuated acrobot. *IEEE Transactions on Robotics and Automation*, 15(4), 740-750.

Din, S.U., Khan, Q., Rehman, F.U., and Akmeliawanti, R. (2017). A comparative experimental study of robust sliding mode control strategies for underactuated systems. *IEEE Access*, 5, 10068-10080.

Fantoni, I. and Lozano, R. (2002). *Non-linear control for underactuated mechanical systems*. Springer Science & Business Media.

Fierro, R., Lewis, F.L., and Lowe, A. (1999). Hybrid control for a class of underactuated mechanical systems. *IEEE Transactions on Systems, Man, and Cybernetics-Part A: Systems and Humans*, 29(6), 649-654.

Ghommam, J., Mnif, F., Benali, A., and Derbel, N. (2006). Asymptotic backstepping stabilization of an underactuated surface vessel. *IEEE Transactions on Control Systems Technology*, 14(6), 1150-1157.

Gruszka, A., Maliso, M., and Mazenc, F. (2011). On tracking for the pvtol model with bounded feedbacks. In *American Control Conference (ACC)*, 2011, 1428-1433. IEEE.

Huang, X. and Yan, Y. (2017). Saturated backstepping control of underactuated spacecraft hovering for

- formation flights. *IEEE Transactions on Aerospace and Electronic Systems*, 53(4), 1988-2000.
- Hwang, C.L., Wu, H.M., and Shih, C.L. (2009). Fuzzy sliding-mode underactuated control for autonomous dynamic balance of an electrical bicycle. *IEEE transactions on control systems technology*, 17(3), 658-670.
- Ichida, K., Watanabe, K., Izumi, K., and Uchida, N. (2006). Fuzzy switching control of underactuated manipulators with approximated switching regions. In *IEEE/RSJ International Conference on Intelligent Robots and Systems*, 2006, 586-591. IEEE.
- Jankovic, M., Fontaine, D., and Kokotovic, P.V. (1996). Tora example: Cascade-and passivity-based control designs. *IEEE Transactions on Control Systems Technology*, 4(3), 292-297.
- Khan, Q., Akmeliawati, R., Bhatti, A.I., and Khan, M.A. (2017). Robust stabilization of underactuated nonlinear systems: A fast terminal sliding mode approach. *ISA transactions*, 66, 241-248.
- Lee, H., & Utkin, V. I. (2007). Chattering suppression methods in sliding mode control systems. *Annual reviews in control*, 31(2), 179-188.
- Lee, S.G. et al. (2013). Sliding mode controls of doublependulum crane systems. *Journal of Mechanical Science and Technology*, 27(6), 1863-1873.
- Levant, A. (2003). Quasi-continuous high-order slidingmode controllers. In *Proceedings. 42nd IEEE Conference on Decision and Control*, 2003., volume 5, 4605-4610. IEEE.
- Li, W., Tanaka, K., and Wang, H.O. (2004). Acrobatic control of a pendubot. *IEEE Transactions on Fuzzy Systems*, 12(4), 549-554.
- Lu, B., Fang, Y., and Sun, N. (2018). Continuous sliding mode control strategy for a class of nonlinear underactuated systems. *IEEE Transactions on Automatic Control*.
- Mason, P., Broucke, M., and Piccoli, B. (2008). Time optimal swing-up of the planar pendulum. *IEEE Transactions on Automatic Control*, 53(8), 1876-1886.
- Nafa, F., Labiod, S., and Chekireb, H. (2013). Direct adaptive fuzzy sliding mode decoupling control for a class of underactuated mechanical systems. *Turkish Journal of Electrical Engineering & Computer Sciences*, 21(6), 1615-1630.
- Olfati-Saber, R. (2001). *Nonlinear control of underactuated mechanical systems with application to robotics and aerospace vehicles*. Ph.D. thesis, Massachusetts Institute of Technology.
- Raguraman, S., Tamilselvi, D., and Shivakumar, N. (2009). Mobile robot navigation using fuzzy logic controller. In *2009 International Conference on Control, Automation, Communication and Energy Conservation, 2009. INCACEC 2009.*, 1-5. IEEE.
- Riachy, S., Orlov, Y., Floquet, T., Santiesteban, R., and Richard, J.P. (2008). Second-order sliding mode control of underactuated mechanical systems i: Local stabilization with application to an inverted pendulum. In *International Journal of Robust and Nonlinear Control: IFAC-Affiliated Journal*, 18(4-5), 529-543.
- Romeo, O., Antonio, L., Johan, N. P., & Hebertt, S. R. (1998). *Passivity-based Control of Euler-Lagrange systems: Mechanical Electrical and Electro-mechanical Applications*. Editorial Springer-Verlag. Great Britain.
- Soysal, B. (2014). Real-time control of an automated guided vehicle using a continuous mode of sliding mode control. *Turkish Journal of Electrical Engineering & Computer Sciences*, 22(5), 1298-1306.
- Spong, M.W., Holm, J.K., and Lee, D. (2007). Passivity-based control of bipedal locomotion. *IEEE Robotics & Automation Magazine*, 14(2), 30-40.
- Tao, C.W., Taur, J.S., Hsieh, T.W., and Tsai, C. (2008). Design of a fuzzy controller with fuzzy swing-up and parallel distributed pole assignment schemes for an inverted pendulum and cart system. *IEEE Transactions on Control Systems Technology*, 16(6), 1277-1288.
- Tsiotras, P. and Luo, J. (2000). Control of underactuated spacecraft with bounded inputs. *Automatica*, 36(8), 1153-1169.
- ud Din, S., ur Rehman, F., and Khan, Q. (2018). Smooth super-twisting sliding mode control for the class of underactuated systems. *PloS one*, 13(10), e0203667.
- Utkin, V., Guldner, J., and Shi, J. (2009). *Sliding mode control in electro-mechanical systems*. CRC press.
- Vazquez, C., Collado, J., and Fridman, L. (2014). Super twisting control of a parametrically excited overhead crane. *Journal of the Franklin Institute*, 351(4), 2283-2298.
- Xiong, J.J. and Zheng, E.H. (2014). Position and attitude tracking control for a quadrotor uav. *ISA transactions*, 53(3), 725-731.
- Yang, E.C.Y., Chao, P.C.P., and Sung, C.K. (2011). Optimal control of an under-actuated system for landing with desired postures. *IEEE Transactions on Control Systems Technology*, 19(2), 248-255.
- Zhang, M. and Tarn, T.J. (2002). Hybrid control of the pendubot. *IEEE/ASME transactions on mechatronics*, 7(1), 79-86.
- Zhao, D., Zhu, Q., and Dubbeldam, J. (2015). Terminal sliding mode control for continuous stirred tank reactor. In *Chemical engineering research and design*, 94, 266-274.
- Zou, Y. (2017). Nonlinear robust adaptive hierarchical sliding mode control approach for quadrotors. *International Journal of Robust and Nonlinear Control*, 27(6), 925-941.